Understanding the Electronic Properties of the Cu_A Site from the Soluble Domain of Cytochrome *c* Oxidase through Paramagnetic ^1H NMR†

Jesús Salgado, Gertrüd Warmerdam, Luigi Bubacco, and Gerard W. Canters*

Leiden Institute of Chemistry, Leiden University, PO Box 9502, 2300 RA Leiden, The Netherlands

Received November 21, 1997; Revised Manuscript Received March 2, 1998

ABSTRACT: The soluble domain of the subunit II of cytochrome *c* oxidase from *Paracoccus versutus* was cloned, expressed, and studied by ^1H NMR at 600 MHz. The properties of the redox-active dinuclear Cu_A site in the paramagnetic mixed-valence Cu(I)−Cu(II) state were investigated in detail. A group of relatively sharp signals found between 30 and 15 ppm in the ^1H NMR spectrum correspond to the imidazole protons of the coordinated histidines (H181 and H224). A second group of broader and farther shifted signals between 50 and 300 ppm are assigned to H^β protons of the bridging cysteines (C216 and C220); the protons from the weak M227 and E218 ligands do not shift outside of the diamagnetic envelope. About 40% of the total spin density appears delocalized over the cysteine-bridging ligands while a much smaller amount is delocalized on the two ligand histidines. The latter have similar spin density distributions. Analysis of the pattern of the hyperfine shifts of the Cys H^β protons shows that the ground state bears $^2B_{3u}$ character, in which the sulfur lobes in the singly occupied molecular orbital are aligned with the Cu−Cu axis. Analysis of the temperature dependence of the shifts of the Cys H^β signals leads to the conclusion that the $^2B_{2u}$ excited state is thermally accessible at room temperature ($\Delta E \approx kT$).

The Cu_A site is a dinuclear copper center with an electron-transfer function. In the state as isolated it has mixed-valence character, and the single unpaired electron is shared by the two copper ions (*1*). One of the main characteristics of the Cu_A is its fast electronic relaxation (*2*−*8*), which allows the observation of relatively narrow hyperfine-shifted lines in the NMR spectra of the paramagnetic species (*6*−*8*). It has been recently shown how this property allows for a powerful spectroscopic investigation of the active site (*6*−*8*). The large isotropic shifts and paramagnetic relaxation experienced by the protons of the coordinated ligands can provide details about the spin delocalization in the site. A careful analysis of these features in the case of the Cu_A center of the cytochrome *c* oxidase from *Paracoccus versutus* is presented in this work.

The Cu_A is found in the subunit II of cytochrome *c* oxidase (COX)[1] (*1*, *9*, *10*). It accepts electrons from cytochrome *c* and donates them to the heme *a* group and the binuclear heme a_3-Cu_B center located in the subunit I (*11*). The other enzyme known to contain a Cu_A site is nitrous oxide reductase (N_2OR) (*12*), where it transfers electrons to the catalytic Cu_Z site which most probably is a dinuclear copper center (*13*). Although the existence of the Cu_A center has been known from the 1960s (*14*, *15*), it is considered a novel metal site because the understanding of its nature, structure, and principal spectroscopic characteristics has come only very recently (*16*−*29*). The structural features of Cu_A are now known from the crystal structures of the bacterial COX from *Paracoccus denitrificans* (*16*, *17*), the bovine mitochondrial COX (*18*, *19*), and the modified, Cu_A-containing, soluble domain of the ubiquinol oxidase from *Escherichia coli*, known as CyoA (*20*). Additionally, careful analysis of extended X-ray absorption fine structure (EXAFS) spectra has contributed to the elucidation of the structural details of the site in both the oxidized and the reduced forms of the Cu_A (*21*, *22*). This metal site is basically defined by a Cu_2S_2 core formed by two copper ions at a ∼2.5-Å distance and two bridging thiolate cysteine sulfurs, these four atoms being located almost in a single plane (*16*, *18*, *20*). Each copper ion is further coordinated by the $N^{\delta 1}$ of a histidine ligand, whose imidazole ring is slightly tilted with regard to the Cu_2S_2 core. The result is an almost symmetric structure, although the (weak) axial ligands are different for the individual copper ions: a methionine sulfur and the peptide carbonyl oxygen from a glutamate (*16*, *18*, *20*) (Chart 1).

The complexity of COX made the study of Cu_A difficult in the past, since the spectroscopic features of this site were partially masked by those of the COX heme centers. These problems were solved with the expression of the soluble

† This work was supported by the Netherlands Foundation for Chemical Research (SON) with financial aid from the Netherlands Organization for Scientific Research (NWO). J.S. thanks the Spanish Ministry of Education and Culture (MEC) for a fellowship.

* Address for correspondence: Leiden Institute of Chemistry, Gorlaeus Laboratories, PO Box 9502, 2300 RA Leiden, The Netherlands. Phone: +31 71 5274256. Fax: +31 71 5274349. E-mail: canters@chem.leidenuniv.nl.

[1] Abbreviations: COX, cytochrome *c* oxidase; CyoA, soluble domain of the subunit II of the quinol oxidase from *Escherichia coli* which was genetically modified to contain the Cu_A site; EXAFS, extended X-ray absorption fine structure; EPR, electron paramagnetic resonance; XAS, X-ray absorption spectroscopy; RR, resonance Raman; Abs, electronic absorption; CD, circular dichroism; MCD, magnetic CD; MO, molecular orbital; SOMO, singly occupied MO; SdII, soluble domain of the subunit II of cytochrome *c* oxidase; WEFT, water-eliminated Fourier transform; 1D, one-dimensional; NOE, nuclear Overhauser enhancement; NOESY, NOE spectroscopy; TPPI, time proportional phase increment.

S0006-2960(97)02859-6 CCC: $15.00
Published on Web 04/28/1998

Chart 1

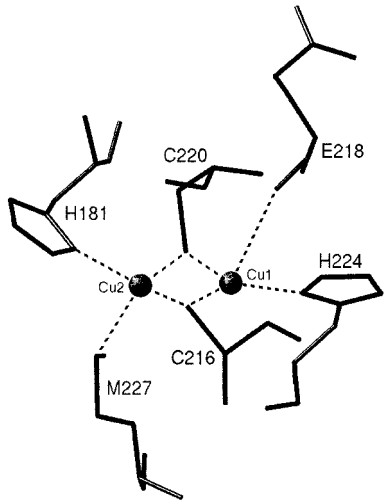

domain of subunit II containing only the Cu_A metal site (*23*−*25*), as well as with the creation of Cu_A containing loop mutants of amicyanin (*26*) and azurin (*27*). The dinuclear, mixed-valence nature of the Cu_A site was suggested by Kroneck and co-workers on the basis of an electron paramagnetic resonance (EPR) investigation of the cupric site of the *Pseudomonas stutzeri* N_2OR, which sieves a fairly well resolved spectrum (*28*). Later on, on the basis of the similarity between the low-frequency EPR spectra of N_2OR and COX, it was proposed that both proteins contain the same type of site (*29*−*31*). A seven-line hyperfine splitting of the EPR spectrum was interpreted as being due to a single unpaired electron interacting with two equivalent copper nuclei (*28*−*31*). From these studies it was established that the Cu_A is a dinuclear highly delocalized mixed-valence class III (*32*) center, which is often denoted as [Cu(1.5)−Cu(1.5)]. Moreover, X-ray absorption spectroscopy (XAS) studies on the *Bacillus subtilis* Cu_A soluble domain led to the suggestion of a direct Cu−Cu interaction in this site (*22*). Such an interaction, unique in biological systems, has been recently supported by far-infrared resonance Raman (RR) spectroscopy studies (*33*) and by the interpretation of electronic absorption (Abs), magnetic circular dichroism (MCD), and sulfur K-edge XAS data (*34*).

The optical spectra are characterized by a broad band at ∼12 000 cm^{-1} and by intense, oppositely signed bands at ∼19 000 and 21 000 cm^{-1} in the MCD (*35*−*38*). When analyzed by Gaussian deconvolution, up to 11 different electronic transitions are found in the region from 33 000 to 7500 cm^{-1} (*38*). Molecular orbital (MO) calculations on models for the Cu_A site and delocalized class III dinuclear copper complexes have led to the qualitative description of the electronic structure of this metal center, which allows the assignment of the electronic spectrum (*38*) and a quantitative interpretation of the EPR spectral properties (*39*). A similar electronic structure is proposed by Solomon and co-workers, who have analyzed the Cu−S and Cu−Cu interactions and defined their contributions to the electronic delocalization in Cu_A (*34*).

The NMR results presented here are interpreted in the framework of the reported electronic structure (*38, 39*). They constitute a new view of the Cu_A site which allows for the unambiguous assignment of the electronic ground state. Additionally, the observed anomalous temperature dependence of the cysteine hyperfine shifts (*6*−*8*) bears witness to the presence of a thermally accessible excited state, suggesting a possible mechanism for the fast electron spin relaxation.

MATERIALS AND METHODS

The Protein Sample. The soluble domain of the cytochrome *c* oxidase from *P. versutus* containing the Cu_A center was obtained as reported for the case of the *P. denitrificans* protein (*10*). A fragment of the gene of subunit II (I. Ciabatti, G. Warmerdam, E. Vijgenboom, and G. W. Canters, unpublished results) corresponding to the C-terminal region of this protein and including residues 128−280 was amplified by PCR, inserted into a pET vector, and overexpressed in *E. coli* BL21 cells. The soluble domain of subunit II (SdII) is obtained in the form of inclusion bodies, which are isolated and reconstituted into properly folded proteins after urea denaturation, followed by dialysis under reducing conditions (0.5 mM DTT) and in the presence of copper (0.2 mM $CuCl_2$) (*10*). Purification of the reconstituted protein was carried out by anionic exchange chromatography on a fast-flow Q-Sepharose column run with a Pharmacia FPLC instrument.

Pure protein samples were checked by UV−vis spectroscopy and EPR and found to show the same spectra as reported for the *P. denitrificans* protein, including a pH transition with a pK_a ∼8.2 (*10*). The purified Cu_A protein used for this study showed a spectral ratio of $A_{280}/A_{480} =$ 13.3 at pH 7.0 and 25 °C.

Samples for NMR spectroscopy were concentrated to 3−5 mM and exchanged for 10 mM sodium phosphate buffer pH 6.5 in either 99.98% or 10% D_2O. pH meter readings of the D_2O samples have not been corrected from the deuterium isotopic effect, and they are denoted by pH*.

NMR Measurements and Calculations. The NMR spectra were recorded on a Bruker DMX 600-MHz spectrometer. 1D NMR spectra, either in H_2O or in D_2O solvent, were measured by using the super-WEFT pulse sequence (*40*). Steady-state 1D NOE measurements were performed as reported in the literature (*41*). NOESY experiments were recorded in the phase-sensitive TPPI mode by using a WEFT-NOESY pulse sequence (*42*).

1D NOE data were analyzed as previously described, using the following equation, valid in the slow motion limit (*43*):

$$\eta_{ij} = -\left(\frac{\mu_0}{4\pi}\right)^2\left(\frac{\hbar^2\gamma_H{}^4\tau_r}{10r_{ij}{}^6\rho_i}\right) \quad (1)$$

where η_{ij} is the NOE observed for signal i upon irradiation of signal j, μ_0 is the magnetic permeability of a vacuum, $\hbar$ is Planck's constant (h) divided by 2π, γ_H is the magnetogyric ratio of the proton, τ_r is the rotational correlation time of the protein, r_{ij} is the distance between the protons i and j, and ρ_i is the longitudinal relaxation rate of proton i.

For the evaluation of the isotropic shifts, the pseudocontact contribution was estimated according to the following equation (*44*):

$$\left(\frac{\Delta\nu}{\nu_0}\right)_{pc} = \left(\frac{\mu_0}{4\pi}\right)\left(\frac{{\mu_B}^2 S(S+1)}{9kT}\right)({g_{||}}^2 - {g_\perp}^2)\left(\frac{3\cos^2\theta - 1}{r^3}\right) \quad (2)$$

$\Delta\nu$ being the hyperfine shift in Hz, ν_0 the resonance frequency of the proton at the magnetic field of the experiment (600 MHz), μ_B the Bohr magneton, S the spin quantum number, k the Boltzmann constant, T the absolute temperature, $g_{||}$ and $g_\perp$ the parallel and perpendicular components of the **g** tensor, θ the angle between the parallel axis of the **g** tensor and the vector connecting the proton and the paramagnetic center, and r the distance between the proton and the paramagnetic center.

The hyperfine contact coupling constants *A/h* (in Hz) were calculated from the following expression (*44*, *45*):

$$\left(\frac{\Delta\nu}{\nu_0}\right)_c = \frac{A}{\hbar}\frac{g_e\mu_B S(S+1)}{3\gamma_H kT} \quad (3)$$

where g_e is the electronic g factor and the rest of the physical constants are defined as above.

The transverse and longitudinal relaxation due to contact coupling were analyzed by using the Solomon−Bloembergen equations (*44*, *46*)

$$T_{2,c}^{-1} = \left(\frac{A}{\hbar}\right)^2\left(\frac{S(S+1)}{3}\right)\left(\tau_e + \frac{\tau_e}{1+{\omega_S}^2{\tau_e}^2}\right) \quad (4)$$

$$T_{1,c}^{-1} = \left(\frac{A}{\hbar}\right)^2\left(\frac{2S(S+1)}{3}\right)\left(\frac{\tau_e}{1+{\omega_S}^2{\tau_e}^2}\right) \quad (5)$$

where τ_e is the electronic correlation time, estimated to be around 2×10^{-11} s for the Cu_A metal center (*8*), and ω_S is the electron Larmor frequency.

Longitudinal dipolar relaxation was analyzed by using the Solomon equation (*47*).

$$T_{1,d}^{-1} = \frac{2}{15}\left(\frac{\mu_0}{4\pi}\right)\left(\frac{{\gamma_H}^2{g_e}^2{\mu_B}^2 S(S+1)}{r^6}\right)\left(\frac{7\tau_c}{1+{\omega_S}^2{\tau_c}^2} + \frac{3\tau_c}{1+{\omega_H}^2{\tau_c}^2}\right) \quad (6)$$

RESULTS

The ^1H NMR Spectrum. The 600-MHz 1D ^1H NMR spectrum of the SdII−Cu_A from *P. versutus* is shown in Figure 1A−C. It displays 10 well-defined downfield shifted signals (a−j), two of them solvent exchangeable (g, h). Some other signals corresponding to exchangeable protons appear resolved in the 12−10 ppm region (Figure 1B, signals k−m), which most likely correspond to backbone amide protons. In the upfield region, no large shifts are observed and only one signal, at −2.1 ppm (n), stands out from the protein (diamagnetic) envelope. More paramagnetic signals are found under the diamagnetic protein envelope. They can be observed in a 10-ms recycle time super-WEFT spectrum recorded in D_2O (Figure 1C, features A−E). The number of protons corresponding to these latter signals is difficult to determine since they consist of various overlapping resonances and their intensity is affected by the strict selection conditions used in the super-WEFT pulse sequence to suppress the diamagnetic signals. However, in inversion−recovery and NOESY experiments (not shown) it can be seen that resonances A−D are composed from different overlapping signals, while signal E probably corresponds to a single methyl group.

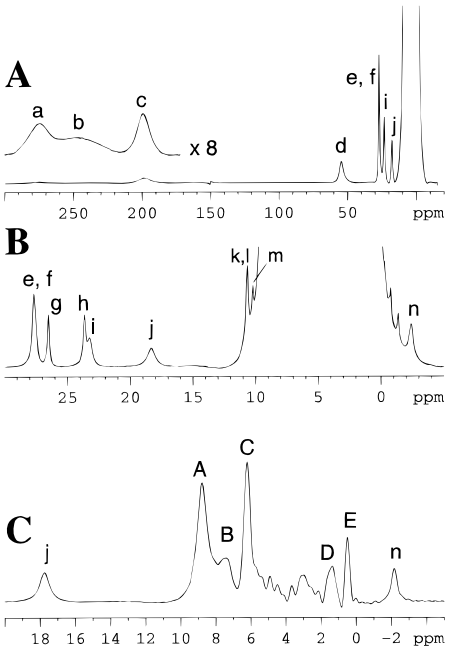

FIGURE 1: 1D ^1H NMR spectra (600-MHz) of the SdII−Cu_A protein measured at 298 K (A, C) and 288 K (B). Sample conditions are 4 mM protein, 10 mM Na_2HPO_4 buffer, in D_2O pH* 6.5 (A, C) or H_2O pH 5.6 (B). All spectra were recorded using a super-WEFT pulse sequence with interpulse delays of 10 ms (A), 50 ms (B), or 5 ms (C). For the spectrum A the carrier frequency was placed at 150 ppm in order to get a sufficient excitation of all resonances.

Signals a−d exhibit similar longitudinal relaxation times, between 0.6 and 1 ms, but their line widths and shifts are quite different. The latter two properties appear to correlate for the four signals a−d (see discussion below), with the exception of the extremely broad signal b. No significant sharpening of the very broad signals a−c was observed when the spectrum was recorded at a lower field (300 MHz, data not shown). Among the moderately shifted signals found between 30 and 16 ppm (Figure 1B), we can distinguish a group of 4 relatively narrow ones, with T_1 values between 14.5 and 9.0 ms (signals e−h), and two other significantly broader ones whose T_1 values are 5.0 ms (i) and 1.8 ms (j). The longitudinal relaxation times of the paramagnetic amide protons k, l, and m are 34.5, 12.5, and 29 ms, respectively, and the upfield shifted signal n has a T_1 of 2.7 ms. The shifts, widths, and relaxation times of the observed paramagnetic signals are summarized in Table 1.

Effect of pH. The NMR spectrum of the SdII−Cu_A is pH dependent between pH 6.5 and 10 (Figure 2). The pH effect is reversible. The intensities of all paramagnetic signals decrease as the pH increases from 6.5, until they eventually vanish at pH > 10. Some small chemical shift variations are also observed. Both the disappearance of the signals and their movement correspond to a ionization process with a pK_a of ∼8.2.

Additionally, it is also observed that signal g disappears at pH > 7.1, and this effect is more pronounced at increasing

Table 1. Chemical Shifts, Relaxation Times, Line Widths, and Assignments of the Paramagnetic Resonances Observed in the ^{1}H NMR Spectrum of SdII−Cu_A[a]

signal	δ (ppm)	T_1 (ms)	$\Delta\nu_{1/2}$ (Hz)	assignment
a	280	1.0 (±0.1)	12 000	C216 $H^{\beta 2}$
b	250	1.0 (±0.5)[b]	25 000	C220 $H^{\beta 2}$
c	200	0.6 (±0.1)	7800	C216 $H^{\beta 1}$
d	54.6	0.7 (±0.1)	1800	C220 $H^{\beta 1}$
e	27.14	14.5 (±0.5)	*c*	H224 $H^{\delta 2}$
f	27.14	14.5 (±0.5)	*c*	H181 $H^{\delta 2}$
g[d]	26.5	9.5 (±0.5)	90	H224 $H^{\epsilon 2}$
h	23.6	9.0 (±0.5)	135	H181 $H^{\epsilon 2}$
i	23.4	5.0 (±0.5)	240	C220 H^{α}
j	17.8	1.8 (±0.1)	195	H224 $H^{\epsilon 1}$
k	10.70	34.6 (±0.2)	*c*	
l	10.48	12.3 (±0.1)	*c*	
m	10.19	29.0 (±0.1)	*c*	
A	8.7	3.0 (±1)[b]	*c*	C216 H^{α}, NH
B	7.4	*c*	*c*	
C	6.2	*c*	*c*	M227 $H^{\beta 1}$
D	1.3	*c*	*c*	
E	0.5	*c*	*c*	
n	−2.1	2.6 (±0.1)	260	M227 $H^{\beta 2}$

[a] Conditions Are 298 K and pH 6.5. [b] Estimated value. [c] Measurement not possible because of overlap. [d] Measured at pH = 5.7 and 288 K.

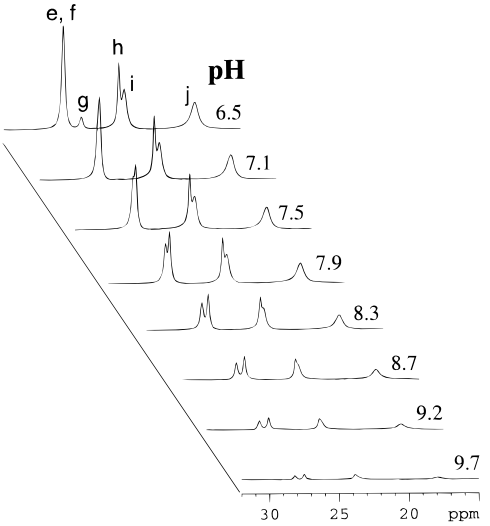

FIGURE 2: pH dependence of the region of the ^{1}H NMR spectrum of SdII−Cu_A containing the histidine signals at 600 MHz and 298 K. The sample was prepared in H_2O without buffer in order to vary pH with minimal additions of diluted NaOH. The values of pH indicated in the figure are averages of the values measured before and after recording the spectrum. The process is reversible and the spectra can be reproduced after reaching pH 10.0 by gradually reducing the pH with small amounts of diluted HCl.

temperature. This phenomenon is of great help for the sequence-specific assignment of the histidine signals, as we shall see below.

Temperature Dependence of the Spectrum. The temperature-dependent variation of the ^{1}H hyperfine shifts of SdII−Cu_A is shown in Figure 3A. A clear anti-Curie temperature dependence is observed for signal d. Additionally, the effect observed for signals a, b, c, and i does not correspond to a pure Curie-type behavior. Thus, signal i is almost temperature insensitive, signal c moves much less than expected for a Curie-type temperature dependence and extrapolates to a very positive δ value (∼135 ppm) at infinite temperature, and signals a and b change more than expected and

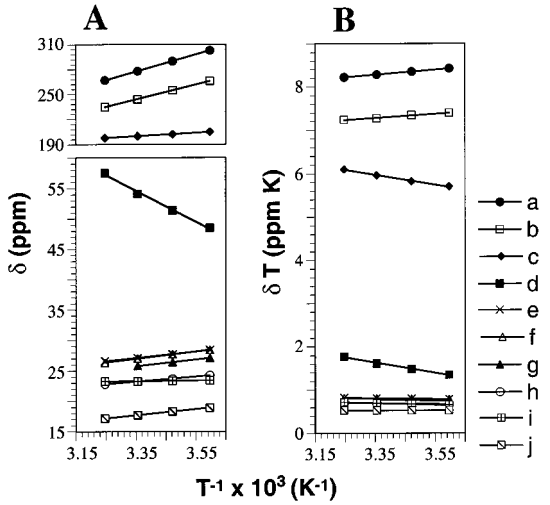

FIGURE 3: Curie plots for SdII−Cu_A at pH 6.5. The values of the hyperfine shifts δ (A) and δT (B) are represented versus $1/T$. Chemical shift data correspond to NMR measurements performed at 278, 288, 298, and 308 K.

extrapolate to positions at infinite temperature in the upfield region (at ∼ −70 and ∼ −50 ppm, respectively) far from their expected diamagnetic position (∼3 ppm). These deviations from the Curie behavior become also evident in a plot of δT vs $1/T$ (Figure 3B), where large slopes are obtained for signals a−d.

Assignment of the ^{1}H Signals. As is usually the case in paramagnetic proteins with coordinated histidines, the labile resonances (g, h) are the starting point for the assignments. They must correspond to the imidazole $N^{\epsilon 2}H$ protons of the two coordinated histidines (H224 and H181[2]) since these are the only exchangeable protons expected to experience large hyperfine shifts. Additionally, proton g exchanges significantly faster with H_2O than proton h (vide supra). This fact is used to assign specifically resonance g to the $N^{\epsilon 2}H$ proton of H224, which, according to the crystal structure of the COX from *P. denitrificans* (*16*), must be exposed to the solvent in the isolated Cu_A soluble domain. Consequently, signal h corresponds to the H181 $N^{\epsilon 2}H$ proton, expected to be buried in the protein matrix and stabilized by a hydrogen bridge with the carboxylate oxygen of D171 (*16*). Signals g and h show NOE connectivities with signals e and f, respectively, in a 10-ms mixing time NOESY spectrum (Figure 4A). Additionally, when the NOESY spectrum is recorded using a 3-ms mixing time, a cross peak is observed between signals g and j (Figure 4B). Such dipolar couplings are expected between vicinal protons in an imidazole ring. Thus, for a histidine coordinated via the $N^{\delta 1}$ nitrogen, NOE connectivities should be detected between the $N^{\epsilon 2}H$ proton and the $C^{\epsilon 1}H$ and $C^{\delta 2}H$ protons. On the other hand, for such $N^{\delta 1}$ coordinated histidines, the $C^{\epsilon 1}H$ proton is located much closer to the paramagnetic center than the $C^{\delta 2}H$ proton, giving rise to much faster relaxing signals. In view of these considerations, signals e and j are assigned to the $C^{\delta 2}H$ and $C^{\epsilon 1}H$ protons, respectively, of H224 and signal f to the $C^{\delta 2}H$ proton of H181.

The most shifted resonances (a−d) are expected to correspond to strongly coordinated residues possessing large

[2] The residue numbers refer to the wild-type subunit II COX sequence.

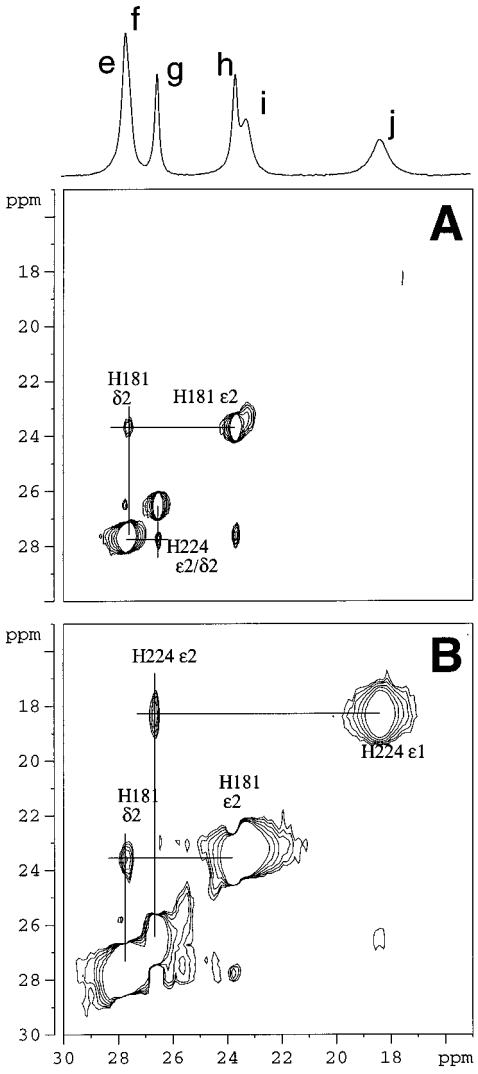

FIGURE 4: WEFT-NOESY spectra (600-MHz) of SdII−Cu_A in H_2O recorded in a 6 mM protein sample at pH 5.6 and 288 K showing the connectivities between the histidine imidazole ring protons. The spectrum in panel A was recorded using a 10-ms mixing time and 84-ms recycle time, while the spectrum in B corresponds to a 3-ms mixing time and 59-ms recycle time.

amounts of unpaired spin density over the donor atoms. The extensive contact couplings associated with these protons are paralleled by their large line widths (see the discussion below). Indeed, similar signals have been observed in the spectrum of the Cu_A soluble domain from *Thermus thermophilus*, where they have been assigned to the coordinated bridging cysteines by specific deuteration of the $C^{\beta}H_2$ protons (*7*). However, no NOEs between these signals have been reported, and their tentative, non-sequence-specific assignment, was based only on the temperature behavior of these protons (*7*). As the T_1 values of signals a−d are around 1 ms (Table 1), by the use of eq 1, a steady-state NOE of ∼2% is expected for pairs of geminal $C^{\beta}H_2$ protons at interproton distances of 1.7 Å when taking into account a correlation time of $\tau_r \approx 10^{-8}$ s (*43*). Such an NOE is indeed observed between signals a and c, as shown in Figure 5A,B, which demonstrates that they must correspond to the same $C^{\beta}H_2$ group of a coordinated cysteine. It follows that signals b and d correspond to the second coordinated Cys residue, although pairing them via NOE was not possible. The large broadening of signal b prevented both its efficient saturation and the observation of the small NOE expected upon saturation of signal d.

A specific assignment of the four Cys β protons is performed, with the help of the low-resolution (2.8-Å) crystal structure of the COX from *P. denitrificans* (*16*), through the analysis of additional NOEs obtained from the irradiation of signals a, c, and d. According to the structure of COX, the $H^{\beta 1}$ of C216 is very close to the $H^{\epsilon 1}$ of H224, assigned above to signal j. An NOE corresponding to signal j is found upon irradiation of signal c (Figure 5C), indicating that this latter resonance arises from the C216 $H^{\beta 1}$ proton, and so signal a corresponds to the $H^{\beta 2}$ proton of the same residue. Consequently, signals b and d are due to the C220 residue. Their specific assignments can be achieved from the interpretation of the NOE between signals d and i (Figure 5E). The latter is not connected to any of the rest of the paramagnetic signals and can be assigned to the α proton of C220. Since this is closer to the C220 $H^{\beta 1}$ proton in the structure of COX (*16*), signal d is assigned to this proton and, consequently, signal b is assigned to the C220 $H^{\beta 2}$ proton. These assignments are supported by the analysis of the dependence of the chemical shifts on the orientation, as we shall explain below.

Additional assignments can be made from the interpretation of other NOEs connecting the Cys and His signals with other protons in the 12 to −5 ppm region. From the irradiation of signals a and c, NOEs are obtained with two of the overlapping resonances in feature A (Figure 5C,D). We assign them to the α and amide protons of C216, both placed in close proximity to the C216−$C^{\beta}H_2$ group. Although the NOE experiment was performed in D_2O, it is well-known that in proteins with a cupredoxin fold many of the amide protons are very protected from exchange and are frequently observed in D_2O samples (*49*). Two additional NOEs are observed by saturation of the C216 $H^{\beta 2}$ proton signal (Figure 5D), corresponding to signals n and C. These signals are in turn connected to each other in a NOESY spectrum (not shown), and signal n is also connected to the C216 $H^{\beta 1}$ proton, (signal c, Figure 5C). From this pattern and according to the structure of COX (*16*), we assign protons C and n to the $H^{\beta 1}$ and $H^{\beta 2}$ protons, respectively, of M227.

DISCUSSION

^{1}H NMR on the Cu_A Site: Comparison with Different Cu_A Proteins. The fast electronic relaxation of Cu_A was reported early in the literature (*2*, *3*). This property allows the observation of relatively sharp NMR resonances in the spectrum of the paramagnetic species, whose isotropic shifts and relaxation contain important information about the structure and electronic properties of the Cu_A center. ^{1}H NMR spectra of three other Cu_A proteins have been reported recently. These are the Cu_A soluble domains of the cytochrome ba_3 from *T. thermophilus* (*7*) and the cytochrome cbb_3 from *B. subtilis* (*6*), and the Cu_A loop-mutant of amicyanin (*6*, *8*). Although the spectra of these proteins are comparable to the one reported here, there are significant differences. The shifts of the Cys H^{β} resonances in the spectrum of the *Thermus* protein are similar to the corresponding shifts in the present spectrum, with the exception of signal d which is significantly more shifted in the case of

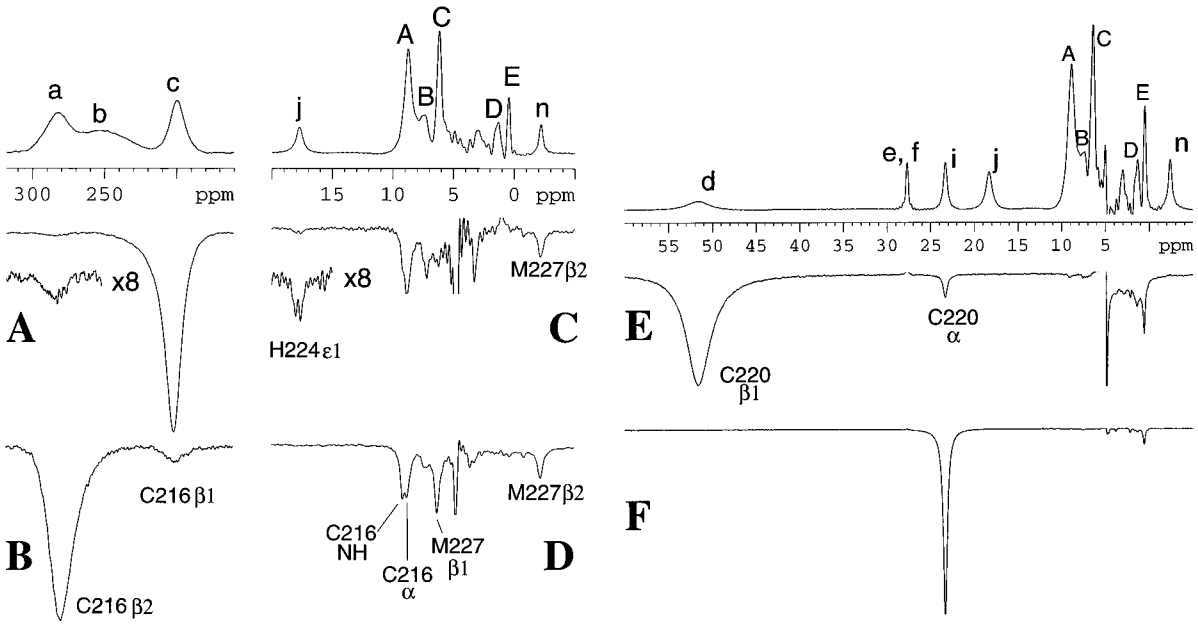

FIGURE 5: Reference and difference spectra from 1D NOE experiments obtained upon irradiation of the Cys signals of SdII−Cu_A in a D_2O sample at pH 6.5 and 298 K. Spectra A and C correspond to the same experiment performed by saturation of signal c with a 15-ms-long decoupling pulse of 32 dB. B and D correspond to the irradiation of signal a using the same conditions. Spectra E and F correspond to the irradiation of signals d and i, respectively.

the *Thermus* Cu_A domain (*7*). This suggests a similar orientation of the Cys side chains with regard to the Cu_2S_2 core in both proteins (see the discussion below). The Cys signals of the *Thermus* and *Paracoccus* proteins also show an analogous temperature dependence. Similar comparisons with the spectra of the *Bacillus* protein and the Cu_A amicyanin are not possible because only one, out of the four Cys β protons, was observed in these two cases.

With regard to the His resonances, they are shifted in the same 15−35 ppm region for the four Cu_A proteins studied by NMR,[3] with the exception of the H181 $H^{\epsilon 1}$ proton which is not observed in the present case, probably because it does not shift outside the diamagnetic envelope. However, when the different His signals are compared in detail we find significant differences. Thus, in the *Paracoccus* and *Thermus* (*7*) proteins, the shifts of the $H^{\delta 2}$ and $H^{\epsilon 2}$ protons corresponding to the two coordinated histidines are similar, while significant differences between the two histidines are observed in the case of the Cu_A amicyanin loop mutant (*8*). As we explain below, this reflects the existence of different degrees of delocalization in different Cu_A centers.

No signals from any of the axial ligands are observed that are significantly shifted outside of the diamagnetic envelope. Indeed, the two proton resonances assigned to the M227 copper ligand are at 6.2 and −2.1 ppm. This is indicative of a very weak interaction of both the M227 and E218 axial ligands with the copper ions and a small or negligible amount of spin density delocalized onto them.

Finally, a singularity of the *P. versutus* Cu_A protein presented here is the pH dependence of the NMR spectrum. No such effect was observed for the three other Cu_A proteins studied by NMR (*6*−*8*). Instead, our observation is analogous to the pH transition studied by UV−vis and EPR spectroscopies for the Cu_A soluble domain of the *P. denitrificans* COX (*10*). In the latter case, it has been reported that the unpaired electron localizes in one of the copper ions at high pH, due to the loss of coordination of the exposed histidine ligand (H224) (*10, 50*). The fact that in the present case no hyperfine-shifted resonances are observed at high pH agrees with the change of Cu_A into a valence-trapped system whose electronic relaxation is too slow to allow the observation of (relatively) sharp shifted resonances. The interconversion from the fast-relaxing (low-pH) species to the slow-relaxing one occurs in the slow exchange limit on the NMR time scale, since no significant broadening of the NMR signals is observed with increasing pH. The small pH-dependent variation of the shifts of some signals, however, does take place in the fast-exchange regime, which indicates that it is connected with a process different from the one causing the disappearance of the shifted signals. Since both exchange phenomena appear to correspond to the same pK_a value, the transition to the localized system may happen through a two-step process. The first one, which is fast on the chemical shift time scale, might be due to a deprotonation, which in turn may trigger a slower transition presumably characterized by a change in the coordination mode of one of the two coppers and the localization of the unpaired spin. The present NMR data allow the identification of neither the residue responsible for the ionization nor the molecular basis for the change of Cu_A into a valence-trapped center.

Spin Density on the His Ligands. The hyperfine shifts of protons from the coordinated residues carry important information about the spin density distribution in the metal site. This information is contained in the Fermi contact term (δ_c) which in order to be analyzed must be separated from the pseudocontact term (δ_{pc}) (*44*). The pseudocontact shift is dipolar in origin and depends on the magnetic anisotropy

[3] Although the signals of the *Bacillus* protein were not assigned, a number of signals with similar characteristics were observed in the 15−35 ppm region (*6*) which are expected to belong to the two coordinated histidines.

Table 2. Contact Shifts, Hyperfine Couplings, and Spin Densities Observed for Protons of the His and Cys Coordinated Residues from the *P. versutus* SdII−Cu_A at 298 K and pH 6.5

signal	δ_c[a] (ppm)	A/h (MHz)	σ_H[b] ($\times 10^3$)
e (H224 $H^{\delta 2}$)	20.1	0.76	0.5
g (H224 $H^{\epsilon 2}$)	15.5	0.58	0.4
j (H224 $H^{\epsilon 1}$)	10.8	0.41	0.3
f (H181 $H^{\delta 2}$)	20.1	0.76	0.5
h (H181 $H^{\epsilon 2}$)	12.6	0.48	0.3
(H181 $H^{\epsilon 1}$)	n.o.[c]		
a (C216 $H^{\beta 2}$)	277	10.5	7.4
c (C216 $H^{\beta 1}$)	197	7.5	5.3
b (C220 $H^{\beta 2}$)	247	9.4	6.6
d (C220 $H^{\beta 1}$)	51.6	2.1	1.5

[a] Diamagnetic shift corrections of 7 ppm for the His $H^{\delta 2}$ protons, 11 ppm for the His $H^{\epsilon 2}$ protons, and 3 ppm for the Cys H^{β} protons were subtracted from the measured chemical shifts. The pseudocontact shift is considered negligible (see the text). [b] Calculated according to $A/h = Q\sigma_H$, with $Q = 1.42 \times 10^3$ MHz (*44*, *52*). [c] Signal probably hidden under the diamagnetic envelope.

of the system, the orientation of the proton with regard to the magnetic axes, and its distance to the paramagnetic center (eq 2) (*44*). To evaluate this contribution, usually the unpaired electron is assumed to be centered on the nucleus of the paramagnetic metal ion (point-dipole approximation). Although for the Cu_A the spin is delocalized on the Cu_2S_2 core, an estimate of the possible interval of values of δ_{pc} can be made by using the reported g values for the Cu_A of the *P. denitrificans* COX ($g_{\|} = 2.180$ and $g_{\perp} = 2.010$) (*10*), a value of 5 Å for the distance r, which is the minimal distance to one of the coppers (*16*, *20*), and values of $(3\cos^2\theta - 1)$ between -1 and 2 (limits corresponding to the extreme cases of $\theta = 90°$ and $\theta = 180°$, respectively). In this way, the pseudocontact shift for the $H^{\delta 2}$ and $H^{\epsilon 2}$ protons of the coordinated histidines is estimated to be $-1.4 \text{ ppm} \leq \delta_{pc} \leq 2.8$ ppm. The magnitude of the limiting values indicates that δ_{pc} can be neglected and that we can equate δ_c with the observed shifts after the subtraction of the diamagnetic shifts (set at 7 ppm for the $H^{\delta 2}$ and $H^{\epsilon 1}$ and 11 ppm for the $H^{\epsilon 2}$, approximate average values found for the Cu(I) derivatives of the related proteins azurin (*49*) and amicyanin (*51*)). From the observed δ_c values and using eq 3, the hyperfine contact coupling constants (A/h) corresponding to the protons of the coordinated histidines have been calculated, and they are listed in Table 2 together with the corresponding proton spin densities. While the hyperfine couplings for the $H^{\delta 2}$ and $H^{\epsilon 2}$ protons are equivalent, the complete shift pattern of the histidine protons (including the $H^{\epsilon 1}$) provides a clear sign that the two histidines are not equivalent. A similar conclusion was reached in the case of a Cu_A amicyanin loop mutant, where significant inequivalence of the two coordinated histidines was found (*8*), although in this latter case the pattern of the chemical shifts of the His residues is different than the one observed here, probably due to structural differences between these two Cu_A forms.

It is interesting to see how the present results compare with those of previous ENDOR measurements on the Cu_A sites of cytochrome *c* oxidases from various sources (mitochondrial yeast or bovine, bacterial) (*53*, *54*). Hoffman and co-workers, as well as others (*53*, *54*), found that the Cu_A center is coordinated by the nitrogens of two histidines exhibiting a fairly isotropic interaction with the unpaired electron in the semireduced site. It was found that the total spin density on the His residues in the Cu_A site is about half of that on the His ligands in the azurin site. The latter observation is confirmed by the present findings: the shifts of the His proton signals from the Cu_A site amount to 15−30 ppm, while, for azurin, contact shifts of twice that magnitude have been observed (*55*).

Table 3. Contact Relaxation for the β Protons of the Cys Bridging Ligands in the *P. versutus* SdII−Cu_A at 298 K and pH 6.5

signal	$(\Delta\nu_{1/2})\pi^a$ (s^{-1})	$(1/T_{2,c})^b$ (s^{-1})	$(1/T_1)^a$ (s^{-1})	$(1/T_{1,c})^b$ (s^{-1})
a (C216 $H^{\beta 2}$)	37 700	25 350	1000	15.4
b (C220 $H^{\beta 2}$)	78 500	20 210	1000	12.3
c (C216 $H^{\beta 1}$)	24 500	12 930	1666	7.8
d (C220 $H^{\beta 1}$)	5650	965	1428	0.5

[a] From experimental data in Table 1. [b] Calculated by using eqs 4 and 5.

Hyperfine Shifts and Relaxation of the Cys β Protons. The four β protons of the coordinated Cys residues display very different shifts ranging from 54.6 to 280 ppm at 298 K. Additionally, they show very different line widths which appear to qualitatively correlate with their shifts (Table 1). As explained above, before the hyperfine shifts are analyzed we have to evaluate the magnitude of the possible pseudocontact contributions. In the case of the Cys ligands, large amounts of spin density are expected to reside in the S^{γ} bridging atoms, due to the extensive spin delocalization over the Cu_2S_2 core. Consequently, to estimate the maximum expected values of δ_{pc}, we have used a lower limit of 2.5 Å for r, corresponding to the approximate distance of any of the Cys H^{β} protons to the closest Cys S^{γ} donor (*16*, *20*). Thus, the pseudocontact contribution is expected to be in the range $-8 \text{ ppm} \leq \delta_{pc} \leq 16$ ppm. This shows that, when neglecting δ_{pc} in the subsequent analysis, only in the case of the C220 $H^{\beta 1}$ proton (signal d) may a non-negligible systematic error be introduced. With regard to the diamagnetic reference position, the average chemical shift of analogous protons in Cu(I) cupredoxins (3 ppm) (*49*, *51*) was used.

The hyperfine contact couplings of the four Cys β protons, calculated from the observed contact shifts at 298 K with eq 3, are collected in Table 2, along with the corresponding proton spin densities (σ_H). From the couplings, and applying eqs 4 and 5, we can also calculate the expected contact contribution to the transverse and longitudinal relaxation rates. The values obtained are listed in Table 3. They show that for the larger shifts (signals a−c) the contact contribution to T_2 is also large and can indeed dominate. The cause for the exceptionally large width of signal b is not clear. One possible explanation is the existence of an equilibrium with an intermediate exchange rate affecting this proton more than the others.

The differences in contact coupling do not affect significantly the relative values of the longitudinal relaxation rates, for which the dipolar term seems to be dominant (Table 3). According to the Solomon equation (*47*), such a dipolar term depends on the sixth power of the distance between the nucleus and the unpaired electron, which is highly delocalized over the Cys S^{γ} donor atoms and the two copper ions. Since the distance of the Cys β protons to the thiolate Cys sulfur of the same residue (~2.5 Å) is much smaller than

the distance to the closest copper ion (3.5−4.2 Å) (*16*, *20*), dipolar relaxation will primarily be dictated by the proton−sulfur distances. As the proton−sulfur distances are similar for the four Cys β protons, similar T_1 values are expected, as is found experimentally.

In theory, the so-called Curie spin relaxation (*48*), arising from the interaction of the nuclear spins with the time-averaged static magnetic moment of the paramagnetic molecule, might contribute to the nuclear relaxation. This is a dipolar contribution which depends, among others, on the square of the applied magnetic field (*48*) and which is responsible for the larger broadenings often observed for paramagnetic proteins at larger fields (*44*, *48*). However, in the present case, no significant sharpening of the signals a−c is obtained when the spectra are recorded at 300 MHz; apparently, the transverse relaxation for these protons is dominated by the large contact and dipolar couplings.

The Couplings of the Cys β Protons and the Electronic Structure of the Cu_A. We have just seen that the four Cys β protons carry very different amounts of spin density (Table 2), and now address the question of the origin of these differences. In a system of the type $M-S^{\gamma}-C^{\beta}H_2-$, where a paramagnetic metal ion, M, is coordinated to a cysteine sulfur, the spin density (or the contact coupling) experienced by the β protons depends on the spin density on the S^{γ} donor atom (ρ_S) and the $M-S^{\gamma}-C^{\beta}-H^{\beta i}$ dihedral angle, $\phi_{\beta i}$. Thus, the contact couplings generally obey a Karplus relationship (*56*−*59*) of the following form:

$$(A_{\beta i}/h) = b \cos^2 \phi_{\beta i} + c \qquad (7)$$

where $i = 1, 2$; $b = B\rho_S$ and $c = C\rho_S$, with B and C constants, and $\phi_{\beta i}$ is measured with respect to the sulfur orbital carrying the unpaired spin density. This equation contains information about both the geometric and the electronic structures of the system. The electronic structure of the Cu_A center has been recently analyzed by Thomson, Kroneck, and co-workers (*38*, *39*). From optical (Abs, CD, and MCD) and EPR spectroscopic data and molecular orbital calculations, they have proposed a $^2B_{3u}$ state to be the ground state of Cu_A, in which the sulfur lobes carrying the unpaired electron in the $3b_{3u}$ singly occupied molecular orbital (SOMO) run parallel to the Cu−Cu axis (Figure 6A,B). However, for the $[Cu_2(L^{iPrdacoS})_2]^+$ mixed-valence, delocalized model complex (*60*), the ground state was found to be $^2B_{2u}$ (*38*, *39*, *62*). In this case the sulfur lobes of the SOMO are collinear with the S−S axis, that is, orthogonal with respect to the $^2B_{3u}$ state (Figure 6B). If we define the angle $\phi_{\beta i}$ relative to the S−S axis (Figure 7), the $A_{\beta i}/h$ coupling will depend on $\cos^2 \phi_{\beta i}$, as expressed in eq 7, for a $^2B_{2u}$ ground state. Alternatively, for a $^2B_{3u}$ ground state the function in eq 7 will be 90° phase-shifted and $A_{\beta i}/h$ will depend on $\sin^2 \phi_{\beta i}$:

$$(A_{\beta i}/h) = b \sin^2 \phi_{\beta i} + c \qquad (8)$$

If we use the $\phi_{\beta i}$ angle values from the crystal structures of COX (*16*) or CyoA (*20*), we can easily verify that qualitatively the pattern of couplings exhibited by the Cys β protons (one small coupling and at least two large ones) is only compatible with a $\sin^2 \phi_{\beta i}$ dihedral angular dependence (Figure 6C). This means that the ground state is $^2B_{3u}$, and

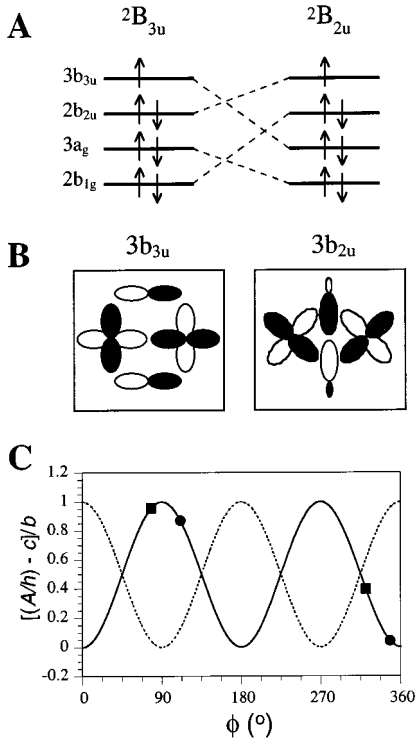

FIGURE 6: (A) Schematic ordering of the four highest energy orbitals (Cu/S antibonding) in the $^2B_{3u}$ and $^2B_{2u}$ states. The ordering is taken from refs 35 and 36. (B) Schematic representation of the SOMO in the $^2B_{3u}$ and $^2B_{2u}$ states (*38*). (C) Variation of the couplings of the β protons from coordinated cysteines with the dihedral angle ϕ (see Figure 7). The continuous line is a $\sin^2$ function and corresponds to the $^2B_{3u}$ state (eq 8). The dotted line is a $\cos^2$ function corresponding to the $^2B_{2u}$ state (eq 7). The values of ϕ from the crystal structures of COX (*16*) and CyoA (*20*) are represented in the plot as squares (C216) and circles (C220).

this, in turn, confirms the assignment of the Cys β protons. A more quantitative analysis is presented below.

Interpretation of the Temperature Dependence of the Cys Hyperfine Shifts: Thermal Accessibility of the Excited State. The abnormal temperature dependence of the cysteine proton shifts (Figure 3) is a characteristic of the Cu_A centers. Thus, a behavior similar to the one reported here has been described for the case of the Cu_A soluble domain of the COX from *T. thermophilus* (*7*) and for the Cu_A amicyanin loop mutant (*8*). There are two possible interpretations for this phenomenon, both implying a temperature variation of the contact coupling constants. In view of the dependence of the couplings of the Cys H^{β} protons on their dihedral angular orientation, the temperature effect could be due to a gradual conformational change connected with a rotation of the Cys side chains around the $S^{\gamma}-C^{\beta}$ bond. As one can deduce from Figure 6C, small shifts in the $\phi_{\beta i}$ angle can produce large or small changes of A/h, of positive or negative sign, depending on the value of this angle and the direction of the shift. Assuming, for calculation purposes, a two-site exchange model and assuming that the crystal structure corresponds to one site (the one which is favored at lower temperatures), the temperature dependence of the shifts of the C216 $C^{\beta}H_2$ protons is compatible with the second site being rotated over −7° with regard to the first site. For the C220, the rotation would amount to −73°. The latter value is too large to be likely, since it would imply dramatic and unrealistic changes in the loop containing C220.

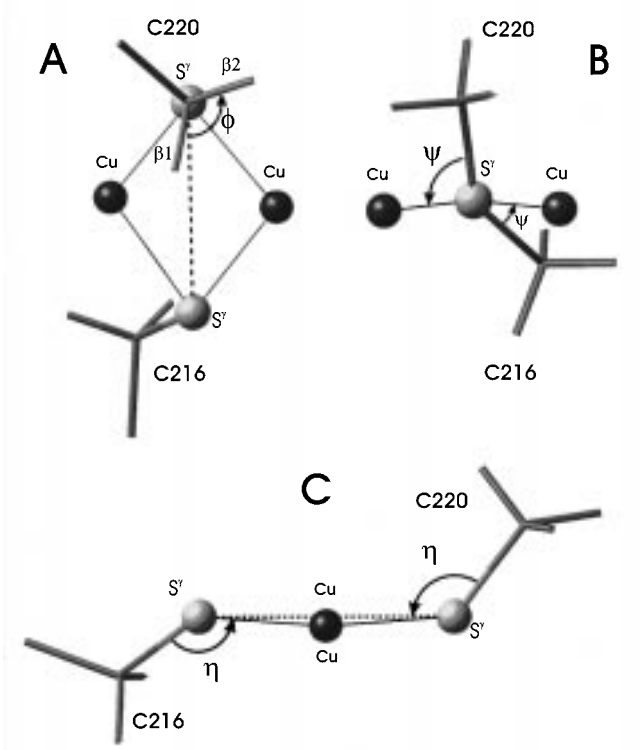

FIGURE 7: Cu_2S_2 core of the Cu_A site viewed down the $C^\beta-S^\gamma$ bond of C220 (A), the $S^\gamma(216)-S^\gamma(220)$ bond (B), and the Cu−Cu axis (C). The orientation of the Cys $H^{\beta i}$ protons is defined relative to the S−S axis through the dihedral angle ϕ, $H^{\beta i}-C^\beta-S^\gamma-S^\gamma$ (A). The position of these protons within the framework of the site is further defined by the dihedral angle ψ, $C^\beta-S^\gamma-S^\gamma-Cu$ (B), and the angle η, $C^\beta-S^\gamma-S^\gamma$ (C). The figures have been produced using the coordinates of the crystal structure of the *P. denitrificans* COX (*16*).

Another explanation is based on the opposite patterns of the Cys H^β contact shifts with $\phi_{\beta i}$ for the $^2B_{3u}$ and $^2B_{2u}$ states and on the assumption that the $^2B_{2u}$ excited state is thermally accessible at room temperature. An increase in the population of the $^2B_{2u}$ state at higher temperatures would result in the increase of the contact shifts of the $H^{\beta 1}$ protons of both C216 and C220 (Figure 6C), which agrees with the negative slopes observed for the plots of the corresponding δT values versus $1/T$ (Figure 3B, signals c and d). On the other hand, in the case of the $H^{\beta 2}$ protons, a smaller coupling is expected as $^2B_{2u}$ gets more populated, again in agreement with the positive slopes of signals a and b in Figure 3B. Thus, the couplings of the cysteine β protons at any temperature can be expressed as an average of the couplings corresponding to the $^2B_{3u}$ and $^2B_{2u}$ states, weighted according to a Boltzmann distribution as follows:

$$\left(\frac{\overline{A}_{\beta i}}{h}\right) = \frac{(b_1 \sin^2 \phi_{\beta i} + c_1) + e^{-\Delta E/kT}(b_2 \cos^2 \phi_{\beta i} + c_2)}{(1 + e^{-\Delta E/kT})} \quad (9)$$

where the subscripts 1 and 2 refer to the ground and excited states, respectively, and the constants b_j and c_j ($j = 1, 2$) are defined (see eq 7) as $B_j\rho_{S,j}$ and $C_j\rho_{Sj}$, respectively.

The couplings of the four cysteine β protons at different temperatures were fitted to eq 9 (Figure 8), with ΔE the same for the two cysteines while $\phi_{\beta 2}$ was set to $\phi_{\beta 1} + 120$, as expected for an ideal sp^3 configuration of the β carbons. The best fit was obtained using $\Delta E = 350\ cm^{-1}$. The values of the dihedral angles $\phi_{\beta i}$ and the parameters b_j and c_j are shown in Table 4. It is worth noticing that there is good agreement between the calculated angles and the crystallographic values collected in the same table. The constants c_j are small compared with b_j, as expected (*56*−*59*). The negative value of c_j for C220 has no physical meaning and may arise from the fact that the small shifts of the C220 $H^{\beta 2}$ (signal d) are sensitive to errors introduced by the approximations made above (like the neglect of the pseudocontact contribution). The values for the constants b_j are significantly different for the two states and for the two cysteine residues. As defined above, b_j is proportional to the S^γ spin density with a proportionality constant B_j. Since the exact values of B_j are not known, it is difficult to state to what extent the differences in b_j represent differences in the spin densities. Values of B have been reported in the literature amounting to ∼100 MHz (*56*). This constant represents the efficiency of the spin density transfer to the $C^\beta H_2$ moiety, which, apart from the dihedral angle $\phi_{\beta i}$, depends on structural factors like, in our case, the orientation of the $C^\beta-S^\gamma$ bond with regard to the Cu−S−S−Cu plane. This orientation can be defined by the dihedral angle ψ, $C^\beta-S^\gamma-S^\gamma-Cu$, and the angle η, $C^\beta-S^\gamma-S^\gamma$ (Figure 7B,C). If we look at the structures of the Cu_A sites available up to date (*16*, *20*), we find that, while η is quite conserved, ψ is significantly different for the two Cys residues, which may be connected with the observed difference in b_j. It is interesting to note that the average value of b for each cysteine is very close to 20 MHz, which would be in agreement with $\rho_S \approx 20\%$ (using $B \approx 100$ MHz (*56*)) for both C216 and C220 (Table 4).

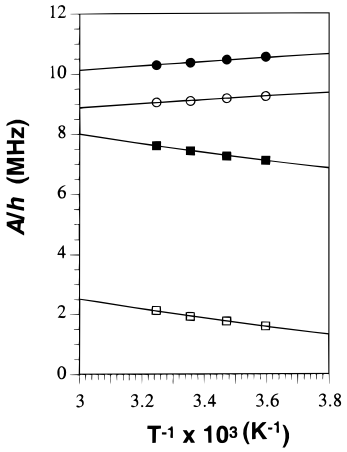

FIGURE 8: Plot of the values of A/h vs $1/T$ and best fit of the data to eq 9. Filled circles correspond to C216 $H^{\beta 2}$, filled squares to C216 $H^{\beta 1}$, open circles to C220 $H^{\beta 2}$, and open squares to C220 $H^{\beta 1}$.

Low-temperature ENDOR studies (*54*, *61*) have revealed the presence of two strongly coupled protons with (anisotropic) couplings that varied, depending on the source of the oxidase, from 12 to 19 MHz. To compare these data with the present results, it must be realized that the ENDOR data refer to the ground state, since at 2.1 K excited states are not populated. With the data in Table 4, the calculated (isotropic) hyperfine couplings for the ground state amount to 11 and 3 MHz and 12 and 0.1 MHz for the C216 and C220, respectively. These data are in complete agreement with the ENDOR data which show the presence of only two strongly coupled protons, and also solve a question posed by Chan and co-workers (*54*) about whether the two strongly coupled protons derive from the same cysteine residue or

Table 4. Dihedral Angles and Constants from Eq 9 Obtained from the Fitting of the Contact Couplings of the Cys β Protons at Different Temperatures (Figure 8)

residue	proton signal	ϕ^a (deg)	ϕ^b (deg)	b_1 (MHz)	b_2 (MHz)	c_1 (MHz)	c_2 (MHz)	b (MHz)	$\rho_S{}^c$
C216	$H^{\beta 2}$ (a)	78 (78)	92	10.3	31.0	0.2	0.5	20.5	0.20
	$H^{\beta 1}$ (c)	−41 (−35)	−28						
C220	$H^{\beta 2}$ (b)	108 (114)	111	14.5	23.8	−0.3	−0.5	19.2	0.19
	$H^{\beta 1}$ (d)	−11 (−12)	−9						

[a] Dihedral angles as defined in Figure 7 measured from the crystal structures of the *P. denitrificans* COX (*16*) and CyoA (between brackets) (*20*). [b] Angles from the fitting using eq 9. [c] From $b = B\rho_S$, assuming $B = 100$ MHz.

from two different ones. Moreover, the isotropic values of 11 and 12 MHz agree nicely with the range of 12−19 MHz observed by ENDOR for the anisotropic couplings.

The value of $\Delta E = 350$ cm^{-1} deserves some comment. This energy is 1 order of magnitude smaller than the value estimated by Farrar et al. (*38*) for the predicted $^2B_{3u} \rightarrow {}^2B_{2u}$ transition (3500 cm^{-1}). Theoretical calculations have shown that the energy difference between the $^2B_{3u}$ and $^2B_{2u}$ states is very sensitive to the Cu−S−Cu angle (a_{1g} deformation) and predict a reversal in the order of the two states at angles in the range 65−70° (*62*). The angles observed in the crystal structures of Cu_A sites (*16, 20*) and determined from EXAFS data (*21*) are inside this interval, which is in agreement with the present value of ΔE. The presence of a low-lying thermally accessible excited state would be compatible with the promotion of electronic relaxation through an Orbach process (*48*).

Finally, a question that deserves further consideration in connection with the energy difference between the $^2B_{3u}$ and $^2B_{2u}$ states being on the order of kT at room temperature relates to the effect of low-lying vibrational states on the spin density distribution. In the resonance Raman spectrum of the Cu_A site, a number of low-frequency vibrations in the 200−400 cm^{-1} region have been identified in the ground state (*63*). The $\upsilon = 0$ and $\upsilon = 1$ levels of these vibrations will carry substantial population at room temperature, and the question is how this may affect the analysis of the temperature dependence of the paramagnetic shifts presented above. It is clear that each vibronic $^2B_{3u}(\upsilon_i)$ level of the ground state will have its $^2B_{2u}(\upsilon_i)$ counterpart in the excited state, and the analysis given above of the temperature dependence of the hyperfine couplings can be simply extended to include excited vibrational states. This will not affect the outcome of the analysis as long as no vibronic mixing occurs. Vibronic mixing is absent, for instance, in the case of totally symmetric vibrations, of which the above-mentioned deformation that causes such a large change in ΔE is an example. The situation is different for vibrations with b_{1g} character (D_{2h} point group), which may in principle lead to coupling between $^2B_{3u}(\upsilon = 1)$ and $^2B_{2u}(\upsilon = 0)$ states. According to the RR analysis, at least two such vibrations with frequencies of 275 and 115 cm^{-1} have been identified (*63*). Vibronic coupling may affect the electronic character of the two levels involved, and thereby the electronic spin distribution. The effect will be pronounced when the states that couple are close in energy. However, in that case their Boltzmann populations will not differ very much and the effects on the thermal average of the hyperfine interactions that result from the vibronic coupling may be compensatory. The net effect, thus, may amount to a small, first-order correction. For a detailed analysis, the magnitude of the vibronic coupling and the details of the electronic wave functions must be known.

CONCLUSIONS

The spin distribution in the Cu_A site is clearly reflected in the ^{1}H NMR spectrum of the paramagnetic one-electron oxidized species. Thus, the shifts of the H181 and H224 proton signals are relatively small but similar to each other, which illustrates the electronic equivalence of the two copper ions. Large amounts of spin density are found in the Cys bridging ligands, as witnessed by the large shifts of the Cys protons. The tentative assignment of the $H^{\beta i}$ protons of Met227 shows that there is a small but sizable amount of spin density delocalized onto this residue.

The spin density in the Cys $H^{\beta i}$ protons depends on the $H^{\beta i}-C^{\beta}-S^{\gamma}-S^{\gamma}$ dihedral angle according to a Karplus-type law. A $^2B_{3u}$ state, with the Cys S^{γ} spin-carrying orbital aligned to the Cu−Cu axis, is assigned as the ground state. The $^2B_{2u}$ excited state is thermally accessible with $\Delta E = 350$ cm^{-1}, which may be connected with the fast relaxation of the Cu_A through an Orbach process.

NOTE ADDED IN PROOF

After submission of this manuscript, a related study appeared (Luchinat, C., Soriano, A., Djinovic-Carugo, K., Saraste, M., Malmström, B. G., and Bertini, I. (1997) *J. Am. Chem. Soc. 119*, 11023−11027). The paper describes a qualitative analysis of the ^{1}H NMR spectrum of the Cu_A soluble domain of cytochrome *c* oxidase from *Paracoccus denitrificans* and deals mainly with the assignment of the signals. The protein is homologous to the one studied here. Although there is, in general, agreement between the two studies as far as the assignments are concerned, some differences in the analysis of the spectral behavior and the assignments of the Cys H^{β} signals are worth commenting upon. Three of the four H^{β} resonances of C216 and C220 were not observed by Luchinat et al. due to problems with the stability of their sample. The shifts of these nuclei were obtained from the deuterium signals of samples with deuterated cysteines, and show a larger spread (up to 450 ppm) than the corresponding resonances in our spectrum. The assignment of these resonances was made only on the basis of their bahavior with temperature and the similarity with the *T. thermophilus* Cu_A protein. As demonstrated here, this can be misleading, since the temperature dependence of the chemical shifts is not as expected on the basis of simple considerations for any of the four Cys H^{β} resonances (see discussion above and plots in Figure 3). In fact, the two Cys H^{β} resonances in our spectra that show an apparent Curie-type behavior (a and b) correspond to different Cys residues.

ACKNOWLEDGMENT

We gratefully acknowledge Professor Hartmut Michel for sending us the coordinates of the COX from *P. denitrificans* and Dr. Matthias Wilmanns and Professor Matti Saraste for the coordinates of the Cu_A CyoA protein. Dr. Frank Neese is acknowledged for sending us his Ph.D. Thesis. Kees Erkelens is acknowledged for his technical assistance with the NMR instrument.

REFERENCES

1. Beinert, H. (1997) *Eur. J. Biochem. 245*, 521−532.
2. Hartzell, C. L., and Beinert, H. (1974) *Biochim. Biophys. Acta 368*, 318−338.
3. Aasa, R., Albracht, S. P. J., Falk, K. E., Lanne, B., and Vänngård, T. (1976) *Biochim. Biophys. Acta 422*, 260−272.
4. Pfenninger, S., Antholine, W. E., Barr, M. E., Hyde, J. S., Kroneck, P. M. H., and Zumft, W. G. (1995) *Biophys. J. 69*, 2761−2769.
5. Mchaourab, H. S., Pfenninger, S., Antholine, W., Felix, C. C., Hyde, J. S., and Kroneck, P. M. H. (1993) *Biophys. J. 64*, 1576−1579.
6. Dennison, C., Berg, A., de Vries, S., and Canters, G. W. (1996) *FEBS Lett. 394*, 340−344.
7. Bertini, I., Bren, K. L., Clemente, A., Fee, J. A., Gray, H. B., Luchinat, C., Malmström, B. G., Richards, J. H., Sanders, D., and Slutter, C. E. (1996) *J. Am. Chem. Soc. 118*, 11658−11659.
8. Dennison, C., Berg, A., and Canters, G. W. (1997) *Biochemistry 36*, 3262−3269.
9. Saraste, M. Q. (1990) *Q. Rev. Biophys. 23*, 331−366.
10. Lappalainen, P., Aasa, R., Malmström, B. G., and Saraste, M. (1993) *J. Biol. Chem. 268*, 26416−26421.
11. Ädelroth, P., Brzezinski, P., and Malmström, B. G. (1995) *Biochemistry 34*, 2844−2849.
12. Zumft, W. G., and Kroneck, P. M. H. (1996) *Adv. Inorg. Biochem. 11*, 193−221.
13. Farrar, J. A., Thomson, A. J., Cheesman, M. R., Dooley, D. M., and Zumft, W. G. (1991) *FEBS Lett. 294*, 11−15.
14. Beinert, H., Griffiths, D. E., Wharton, D. C., and Sanders, R. H. (1962) *J. Biol. Chem. 237*, 2337−2346.
15. Griffiths, D. E., and Wharton, D. C. (1961) *J. Biol. Chem. 236*, 1850−1856.
16. Iwata, S., Ostermeier, C., Ludwig, B., and Michel, H. (1995) *Nature 376*, 660−669.
17. Ostermeier, C., Harrenga, A., Ermler, U., and Michel, H. (1997) *Proc. Natl. Acad. Sci. U.S.A.* 94, 10547−10553.
18. Tsukihara, T., Aoyama, H., Yamashita, E., Tomizaki, T., Yamaguchi, H., Shinzawa-Itoh, K., Nakashima, R., Yaono, R., and Yoshikawa, S. (1995) *Science 269*, 1069−1074.
19. Tsukihara, T., Aoyama, H., Yamashita, E., Tomizaki, T., Yamaguchi, H., Shinzawa-Itoh, K., Nakashima, R., Yaono, R., and Yoshikawa, S. (1996) *Science 272*, 1136−1144.
20. Wilmanns, M., Lappalainen, P., Kelly, M., Sauer-Eriksson, E., and Saraste, M. (1995) *Proc. Natl. Acad. Sci. U.S.A. 92*, 11955−11959.
21. Blackburn, N. J., de Vries, S., Barr, M. E., Houser, R. P., Tolman, W. B., Sanders, D., and Fee, J. A. (1997) *J. Am. Chem. Soc. 119*, 6135−6143.
22. Blackburn, N. J., Barr, M. E., Woodruff, W. H., van der Oost, J., and de Vries, S. (1994) *Biochemistry 33*, 10401−10407.
23. van der Oost, J., Lappalainen, P., Mussacchio, A., Warne, A., Lemieux, L., Rumbley, J., Gennis, R. B., Aasa, R., Pascher, T., Malmström, B. G., and Saraste, M. (1992) *EMBO J. 11*, 3209−3217.
24. von Wachenfeldt, C., de Vries, S., and van der Oost, J. (1994) *FEBS Lett. 340*, 109−113.
25. Slutter, C. E., Sanders, D., Wittung, P., Malmström, B. G., Aasa, R., Richards, J. H., Gray, H. B., and Fee, J. A. (1996) *Biochemistry 35*, 3387−3395.
26. Dennison, C., Vijgenboom, E., de Vries, S., van der Oost, J., and Canters, G. W. (1995) *FEBS Lett. 365*, 92−94.
27. Hay, M., Richards, J. H., and Lu, Y. (1996) *Proc. Natl. Acad. Sci. U.S.A. 93*, 461−464.
28. Kroneck, P. M. H., Antholine, W. E., Riester, J., and Zumft, W. G. (1988) *FEBS Lett. 242*, 70−74.
29. Kroneck, P. M. H., Antholine, W. E., Riester, J., and Zumft, W. G. (1989) *FEBS Lett. 248*, 212−213.
30. Kroneck, P. M. H., Antholine, W. E., Kastrau, D. H. W., Buse, G., Steffens, G. C. M., and Zumft, W. G. (1990) *FEBS Lett. 268*, 274−276.
31. Antholine, W. E., Kastrau, D. H. W., Steffens, G. C. M., Buse, G., Zumft, W. G., and Kroneck, P. M. H. (1992) *Eur. J. Biochem. 209*, 875−881.
32. Robin, M. B., and Day, P. (1967) *Adv. Inorg. Chem. Radiochem. 10*, 247−422.
33. Wallace-Williams, S. E., James, C. A., de Vries, S., Saraste, M., Lappalainen, P., van der Oost, J., Fabian, M., Palmer, G., and Woodruff, W. H. (1996) *J. Am. Chem. Soc. 118*, 3986−3987.
34. Williams, K. R., Gamelin, D. R., LaCroix, L. B., Houser, R. P., Tolman, W. B., Mulder, T. C., de Vries, S., Hedman, B., Hodgson, K. O., and Solomon, E. I. (1997) *J. Am. Chem. Soc. 119*, 613−614.
35. Thomson, A. J., Greenwood, C., Peterson, J., and Barrett, C. P. (1986) *J. Inorg. Biochem. 28*, 195−205.
36. Greenwood, C., Hill, B. C., Barber, D., Eglinton, D. G., and Thomson, A. J. (1983) *Biochem. J. 215*, 303−316.
37. Dooley, D. M., McGuirl, M. A., Rosenzweig, A. C., Landin, J. A., Scott, R. A., Zumft, W. G., Devlin, F., and Stephens, P. J. (1991) *Inorg. Chem. 30*, 3006−3011.
38. Farrar, J. A., Neese, F., Lappalainen, P., Kroneck, P. M. H., Saraste, M., Zumft, W. G., and Thomson, A. J. (1996) *J. Am. Chem. Soc. 118*, 11501−11514.
39. Neese, F., Zumft, W. G., Antholine, W. E., and Kroneck, P. M. H. (1996) *J. Am. Chem. Soc. 118*, 8692−8699.
40. Inubushi, T., and Becker, E. D. (1983) *J. Magn. Reson. 51*, 128−133.
41. Banci, L., Bertini, I., Luchinat, C., and Piccioli, M. (1990) *FEBS Lett. 272*, 175−180.
42. Chen, Z., de Ropp, J. S., Hernández, G., and La Mar, G. N. (1994) *J. Am. Chem. Soc. 116*, 8772−8783.
43. Banci, L., Bertini, I., and Luchinat, C. (1991) in *NMR and biomolecular structure* (Bertini, I., Molinari, H., and Niccolai, N., Eds.) p 31, VCH, Weinheim.
44. Bertini, I., and Luchinat, C. (1996) *Coord. Chem. Rev. 150*, 1−296.
45. Bloembergen, N. (1957) *J. Chem. Phys. 27*, 595−596.
46. Solomon, I., and Bloembergen, N. (1956) *J. Chem. Phys. 25*, 261−266.
47. Solomon, I. (1955) *Phys. Rev. 99*, 559−565.
48. Banci, L., Bertini, I., and Luchinat, C. (1991) *Nuclear and electron relaxation*, VCH, Weinheim.
49. van de Kamp, M., Canters, G. W., Wijmenga, S. S., Lommen, A., Hilbers, C. W., Nar, H., Messerschmidt, A., and Huber, R. (1992) *Biochemistry 31*, 10194−10207.
50. Farrar, J. A., Lappalainen, P., Zumft, W. G., Saraste, M., and Thomson, A. J. (1995) *Eur. J. Biochem. 232*, 294−303.
51. Lommen, A., Wijmenga, S. S., Hilbers, C. W., and Canters, G. W. (1991) *Eur. J. Biochem. 201*, 695−702.
52. Beringer, R., and Heald, M. A. (1954) *Phys. Rev. 95*, 1474−1481.
53. Gurbiel, R. J., Fann, Y. C., Surerus, K. K., Werst, M. M., Musser, S. M., Doan, P. E., Chan, S. I., Fee, J. A., and Hoffman, B. M. (1993) *J. Am. Chem. Soc. 115*, 10888−10894.
54. Stevens, T. H., Martin, C. T., Wang, H., Brudvig, W., Scholes, C., and Chan, S. (1982) *J. Biol. Chem. 257*, 12106−12113.
55. Kalverda, A. P., Salgado, J., Dennison, C., & Canters, G. W. (1996) *Biochemistry 35*, 3085−3092.
56. Werst, M. M., Davoust, C. E., and Hoffman, B. M. (1991) *J. Am. Chem. Soc. 113*, 1533−1538.
57. Ho, F. F. L., and Reilley, C. N. (1969) *Anal. Chem. 41*, 1835−1841.
58. Bertini, I., Capozzi, F., Luchinat, C., Piccioli, M., and Vila, A. J. (1994) *J. Am. Chem. Soc. 116*, 651−660.
59. Karplus, M. (1959) *J. Chem. Phys. 30*, 11−15.

60. Houser, R. P., Young, V. G., and Tolman, W. B. (1996) *J. Am. Chem. Soc. 118*, 2101−2102.
61. van Camp, H. L., Wei, Y. H., Scholes, C. P., and King, T. E. (1978) *Biochim. Biophys. Acta 537*, 238−246.
62. Neese, F. (1996) Ph.D. Thesis, University of Konstanz.
63. andrew, C. R., Fraczkiewicz, R., Czernuszewicz, R. S., Lappalainen, P., Saraste, M., and Sanders-Loehr, J. (1996) *J. Am. Chem. Soc. 118*, 10436−10445.

BI9728598